



Research article

On the nonstandard numerical discretization of SIR epidemic model with a saturated incidence rate and vaccination

Agus Suryanto and Isnani Darti*

Department of Mathematics, Faculty of Mathematics and Natural Sciences, University of Brawijaya, Malang 65145, Indonesia

* **Correspondence:** Email: isnaniidarti@ub.ac.id.

Abstract: Recently, Hoang and Egbelowo (Boletin de la Sociedad Matemática Mexicana, 2020) proposed a nonstandard finite difference scheme (NSFD) to get a discrete SIR epidemic model with saturated incidence rate and constant vaccination. The discrete model was derived by discretizing the right-hand sides of the system locally and the first order derivative is approximated by the generalized forward difference method but with a restrictive denominator function. Their analysis showed that the NSFD scheme is dynamically-consistent only for relatively small time-step sizes. In this paper, we propose and analyze an alternative NSFD scheme by applying nonlocal approximation and choosing the denominator function such that the proposed scheme preserves the boundedness of solutions. It is verified that the proposed discrete model is dynamically-consistent with the corresponding continuous model for all time-step size. The analytical results have been confirmed by some numerical simulations. We also show numerically that the proposed NSFD scheme is superior to the Euler method and the NSFD method proposed by Hoang and Egbelowo (2020).

Keywords: SIR epidemic model; saturated incidence rate; local and global stability analysis; Lyapunov function; dynamically-consistent discretization

Mathematics Subject Classification: 92D30, 37N25, 39A30

1. Introduction

Over recent decades, mathematical models are considered as crucial tools for understanding the transmission mechanism and evaluating the control strategies of infectious diseases, see [1–3]. In this respect, Yusuf and Benyah [4] have introduced and analyzed a SIR epidemic model with constant vaccination and treatment where the incidence rate is assumed to be bi-linear. The bi-linear incidence rate describes that disease transmission is proportional to the number of susceptible individuals and infective individuals, and so the greater the number of susceptible individuals and infective individuals

cause an even greater transmission rate. Hence the bi-linear incidence rate is not realistic for cases in a large population since there are changes in the social and psychological behavior of society or some prevention measure taken by the society which reduce the transmission rates. To deal with the crowding effect or behavioral change, Capasso and Serio [5] proposed a saturated incidence rate $\frac{\beta SI}{1+\alpha I}$ where β is the maximal disease transmission rate and α is the saturation factor that measures the inhibitory effect due to the crowding effect or behavioral change of society [6]. After that, the saturated incidence rate has been widely applied to deterministic epidemic models [7–10], epidemic models with optimal control [11–13] or stochastic epidemic models [14–16]. If the bilinear incidence rate in the SIR epidemic model [4] is replaced by the saturated incidence rate, then we get

$$\begin{aligned}\frac{dS}{dt} &= \Lambda - \frac{\beta SI}{1 + \alpha I} - (\nu + \mu)S \\ \frac{dI}{dt} &= \frac{\beta SI}{1 + \alpha I} - (\mu + \gamma + \delta)I \\ \frac{dR}{dt} &= \nu S + \gamma I - \mu R,\end{aligned}\tag{1.1}$$

where $S \equiv S(t)$, $I \equiv I(t)$ and $R \equiv R(t)$ denote the sub-population of susceptible, infective, and recovered at time t , respectively. Λ , ν and γ are positive parameters which respectively represent the recruitment rate of population, vaccination rate, and recovery rate due to treatment. The natural death rate and the death rate induced by the disease are respectively denoted by μ and δ . It is assumed that initial values are non-negativity: $S(0) = S_0 \geq 0$, $I(0) = I_0 \geq 0$ and $R(0) = R_0 \geq 0$. Recently, the SIR model (1.1) has been applied by Khan et al. [17] to model the spread of hepatitis B virus. The local and global stability analysis of the disease free equilibrium (DFE) point were established, but the disease endemic equilibrium (DEE) point was only studied locally. The global stability analysis of the DEE point of the model was then provided by Hoang and Egbeowo [18]. Very recently, Macías-Díaz et al. [19] studied the diffusion effect on the spread of the hepatitis B virus.

The mathematical epidemic models are generally in the form of a nonlinear differential equations system so that their analytical solutions are difficult to be obtained. Hence numerical approximations are often needed to get reliable results. However, it was shown that many standard numerical methods such as the Euler method, Runge-Kutta method, and other standard finite difference methods may fail to maintain the dynamical properties of the corresponding continuous models, see e.g. [20–22]. To overcome such dynamics-inconsistency, Mickens [23] has developed a nonstandard finite difference (NSFD) method. A numerical scheme for a system of first-order differential equations is called an NSFD scheme if at least one of the following conditions is satisfied.

- The first-order derivatives in the system are approximated by the generalized forward difference method

$$\frac{du_n}{dt} \approx \frac{u_{n+1} - u_n}{\phi},$$

where $u_n = u(t_n)$ and $\phi \equiv \phi(h)$ is the denominator function such that $\phi(h) = h + O(h^2)$ and h is the time-step size.

- The nonlinear terms are approximated non-locally. For example $u^2(t_n) \approx u_n u_{n+1}$.

The NSFD method has been successfully implemented in various problems such as epidemiology [24–30], ecology [28,31–33] or metapopulation model [34]. However, we notice that an NSFD scheme

for a differential equation is not unique. Hence, the dynamical properties of an NSFD scheme need to be analyzed to ensure whether an NSFD scheme maintains the dynamics-consistency with its original continuous equation or not. NSFD schemes in [27, 28, 31–33] did not apply the generalized forward difference method but they used nonlocal approximation. Moreover, the authors in those references did not consider the population conservation law. Their dynamical analysis shows that the NSFD schemes in [27, 31, 32] maintain the stability properties of all existing equilibrium points irrespective of the time-step size (h). However, the NSFD schemes in [28, 33] require a relatively small h for the stability of equilibrium points. Cui et al. [24–26] and the authors in [29, 30] applied both generalized forward difference method and nonlocal approximation. They have proven that the obtained NSFD schemes preserve all dynamical properties of the corresponding continuous models irrespective of h . In particular, the denominator function must be appropriately chosen to satisfy the exact population conservation law.

Recently, Hoang and Egbelowo [18] proposed a numerical scheme for the model (1.1) to get the following discrete model

$$\begin{aligned}\frac{S_{n+1} - S_n}{\phi} &= \Lambda - \frac{\beta S_n I_n}{1 + \alpha I_n} - (\mu + \nu)S_n \\ \frac{I_{n+1} - I_n}{\phi} &= \frac{\beta S_n I_n}{1 + \alpha I_n} - (\mu + \gamma + \delta)I_n \\ \frac{R_{n+1} - R_n}{\phi} &= \nu S_n + \gamma I_n - \mu R_n,\end{aligned}\tag{1.2}$$

where ϕ is any denominator function but it must obey $\phi \equiv \phi(h) = h + O(h^2)$. Notice that the NSFD scheme (1.2) implements the generalized forward method and a local approximation for the right-hand sides. Rigorous investigation on the dynamical properties shows that the discrete model (1.2) preserves the dynamics-consistency of the model (1.1) only if the denominator function satisfies $\phi(h) < \phi^*$, where ϕ^* is a critical value of the denominator function which is determined by some parameters in the model (1.1). Hence, the preservation of dynamics-consistency is achieved only when the time-step size is relatively small.

In this paper, we propose an alternative NSFD scheme for the model (1.1) which is dynamically-consistent with the original continuous model for any time-step size. Following Cui et al. [24–26, 29, 30], we apply both the generalized forward difference method and nonlocal approximation to construct the NSFD scheme. We organize the rest of the paper as follows. In Section 2 we review the dynamical properties of model (1.1) based on the analytical results in [17, 18]. The derivation of the NSFD scheme for model (1.1) is presented in Section 3. We show in this section that the obtained discrete NSFD model has the same dynamical properties as the corresponding continuous model. To illustrate our analytical findings, we present numerical simulations in Section 4. We draw some conclusions in the final section.

2. Dynamics of the continuous epidemic model

As for other models of population dynamics, the SIR epidemic model with a saturated incidence rate (1.1) is required to have positive and bounded solutions. The positivity of the solution of model (1.1) has been proven in [17] and is stated in the following theorem.

Theorem 1. [17] *If the solution of the SIR epidemic model (1.1) subject to non-negative initial values exist, then it is positive $\forall t > 0$.*

The boundedness of the solution is related to limited resources so that the population cannot grow infinitely. Hence, the boundedness of the solution of model (1.1) is biologically important but it has not been described in [17, 18]. In the following theorem, we establish the boundedness of solution for the model (1.1).

Theorem 2. *The solution of the SIR epidemic model (1.1) subject to non-negative initial values is ultimately bounded.*

Proof. Let $P(t) = S(t) + I(t) + R(t)$ be the total population. From model (1.1) we have

$$\frac{dP}{dt} = \Lambda - \mu P - \delta I \leq \Lambda - \mu P, \quad (2.1)$$

from which we get

$$P(t) \leq \frac{\Lambda}{\mu} + \left(P_0 - \frac{\Lambda}{\mu}\right) \exp(-\mu t), \quad (2.2)$$

where $P_0 = S_0 + I_0 + R_0$. It is clear that $\lim_{t \rightarrow +\infty} P(t) \leq \frac{\Lambda}{\mu}$, and thus $S(t)$, $I(t)$ and $R(t)$ are ultimately bounded. \square

From Theorem 1 and Theorem 2, we see that model (1.1) has a feasible region

$$\Omega = \{(S, I, R) : 0 \leq S + I + R \leq \frac{\Lambda}{\mu}, S \geq 0, I \geq 0, R \geq 0\},$$

which is positively invariant. Therefore, the SIR epidemic model (1.1) is mathematically and epidemiologically well posed in Ω .

Using the next generation matrix method, Khan et al. [17] derived the basic reproduction number for model (1.1), namely

$$\mathcal{R}_0 = \frac{\Lambda\beta}{(\mu + \nu)(\mu + \gamma + \delta)}. \quad (2.3)$$

It was also shown in [17] that model (1.1) always has a DFE point $E^0 = (S^0, 0, R^0)$, where $S^0 = \frac{\Lambda}{\mu + \nu}$ and $R^0 = \frac{\Lambda\nu}{\mu(\mu + \nu)}$. In addition to the DFE point, if $\mathcal{R}_0 > 1$, then model (1.1) also has a DEE point $E^* = (S^*, I^*, R^*)$ where $S^* = \frac{\alpha\Lambda + (\mu + \gamma + \delta)}{\alpha(\mu + \nu) + \beta}$, $I^* = \frac{(\mu + \nu)(\mathcal{R}_0 - 1)}{\alpha(\mu + \nu) + \beta}$ and $R^* = \frac{\nu S^* + \gamma I^*}{\mu}$. The following theorem about the stability of the DFE and DEE points are taken from [17, 18].

Theorem 3. [17]

1. *The DFE point of model (1.1) is locally asymptotically stable if $\mathcal{R}_0 < 1$ and it is unstable if $\mathcal{R}_0 > 1$.*
2. *The DEE point of model (1.1) is locally asymptotically stable if $\mathcal{R}_0 > 1$.*

Theorem 4. [18]

1. *The DFE point of model (1.1) is globally asymptotically stable if $\mathcal{R}_0 \leq 1$.*
2. *The DEE point of model (1.1) is globally asymptotically stable if $\mathcal{R}_0 > 1$.*

3. Dynamically-consistent NSFD discretization of the SIR epidemic model with saturated incidence rate and vaccination

3.1. Construction of the NSFD scheme

For the rest of this paper, we respectively denote S_n, I_n and R_n as the numerical approximation of $S(t), I(t)$ and $R(t)$ at $t = nh, n = 0, 1, 2, \dots$, where h is the time-step size. Using the idea of Mickens [23], we discretize model (1.1) as follows

$$\begin{aligned}\frac{S_{n+1} - S_n}{\phi} &= \Lambda - \frac{\beta S_{n+1} I_n}{1 + \alpha I_n} - (\mu + \nu) S_{n+1} \\ \frac{I_{n+1} - I_n}{\phi} &= \frac{\beta S_{n+1} I_n}{1 + \alpha I_n} - (\mu + \gamma + \delta) I_{n+1} \\ \frac{R_{n+1} - R_n}{\phi} &= \nu S_{n+1} + \gamma I_{n+1} - \mu R_{n+1}.\end{aligned}\quad (3.1)$$

The initial values of the discrete NSFD SIR epidemic model (3.1) are also supposed to be non-negative: $S_0 \geq 0, I_0 \geq 0$ and $R_0 \geq 0$. Different from the scheme (1.2), the NSFD scheme (3.1) approximates the nonlinear terms in the right-hand sides nonlocally. Furthermore, the denominator function ϕ in (3.1) is not arbitrary, but it will be derived such that it obeys the exact boundedness of solutions. To do so, we denote the total population as $P_n = S_n + I_n + R_n$. From the discrete NSFD model (3.1), we have

$$\frac{P_{n+1} - P_n}{\phi} = \Lambda - \mu P_{n+1} - \delta I_{n+1} \leq \Lambda - \mu P_{n+1}.\quad (3.2)$$

By straightforward calculations, it is easy to verify that if we take a denominator function

$$\phi = \frac{\exp(\mu h) - 1}{\mu},\quad (3.3)$$

then the solution of equation (3.2) satisfies

$$P_n \leq \frac{\Lambda}{\mu} + \left(P_0 - \frac{\Lambda}{\mu}\right) \exp(-\mu n h),\quad (3.4)$$

for any $h > 0$. Additionally, for the case of $\delta = 0$, we can also show that the total population of the discrete NSFD model (3.1) are exactly the same as that of model (1.1). Hence, the discrete NSFD model (3.1) maintains the exact boundedness of solutions (2.2). The discrete NSFD model (3.1) can be rearranged to get explicit form

$$\begin{aligned}S_{n+1} &= \frac{S_n + \phi \Lambda}{1 + \phi(\mu + \nu + \Psi_n)} \\ I_{n+1} &= \frac{I_n + \phi \Psi_n S_{n+1}}{1 + \phi(\mu + \gamma + \delta)} \\ R_{n+1} &= \frac{R_n + \phi(\nu S_{n+1} + \gamma I_{n+1})}{1 + \phi \mu},\end{aligned}\quad (3.5)$$

where $\Psi(z) = \frac{\beta z}{1+\alpha z}$ and $\Psi_n = \Psi(I_n)$. Since all parameters in (3.5) are positive, it is proven that $S_n \geq 0$, $I_n \geq 0$ and $R_n \geq 0$ for all $n > 0$ and for any $h > 0$. This finding confirms the discrete NSFD model (3.5) preserves the non-negativity solutions for any h .

By applying some algebraic calculations, we can easily verify that the discrete NSFD model (3.5) has exactly the same equilibrium points as continuous model (1.1), namely the DFE point $E^0 = (S^0, 0, R^0)$ and the DEE point $E^* = (S^*, I^*, R^*)$. The DEE point E^* exists if $\mathcal{R}_0 > 1$. The local and global stability of equilibrium point E^0 and E^* are investigated in the following Subsections.

3.2. Local stability analysis of the discrete NSFD model

By noticing that the first two equations in the discrete NSFD model (3.5) do not depend on the third equation, the stability analysis can be performed by considering the following reduced model

$$\begin{aligned} S_{n+1} &= \frac{S_n + \phi\Lambda}{1 + \phi(\mu + \nu + \Psi_n)} = F_1(S, I) \\ I_{n+1} &= \frac{I_n + \phi\Psi_n S_{n+1}}{1 + \phi(\mu + \gamma + \delta)} = F_2(S, I). \end{aligned} \quad (3.6)$$

The Jacobian matrix of the discrete NSFD model (3.6) at a point $\bar{E} = (\bar{S}, \bar{I})$ is given by

$$J(\bar{S}, \bar{I}) = \begin{pmatrix} \frac{\partial F_1}{\partial S}(\bar{S}, \bar{I}) & \frac{\partial F_1}{\partial I}(\bar{S}, \bar{I}) \\ \frac{\partial F_2}{\partial S}(\bar{S}, \bar{I}) & \frac{\partial F_2}{\partial I}(\bar{S}, \bar{I}) \end{pmatrix}. \quad (3.7)$$

By observing the eigenvalues of the Jacobian matrix $J(\bar{S}, \bar{I})$, we study the local stability of equilibrium points as in the following theorems.

Theorem 5. *If $\mathcal{R}_0 < 1$, then the DFE point E^0 of the discrete NSFD model (3.6) is locally asymptotically stable for all $h > 0$. Furthermore, if $\mathcal{R}_0 > 1$ then E^0 is unstable for all $h > 0$.*

Proof. If we substitute the DFE point E^0 into the Jacobian matrix (3.7), then we get

$$J(E^0) = \begin{pmatrix} \frac{1}{1+\phi(\mu+\nu)} & -\frac{\phi\beta(S^0+\phi\Lambda)}{(1+\phi(\mu+\nu))^2} \\ 0 & \frac{\mu+\nu+\phi\Lambda\beta}{\mu+\nu+\phi(\mu+\nu)(\mu+\gamma+\delta)} \end{pmatrix}. \quad (3.8)$$

The eigenvalues of $J(E^0)$ are obviously

$$0 < \lambda_1 = \frac{1}{1 + \phi(\mu + \nu)} < 1 \quad \text{and} \quad \lambda_2 = \frac{\mu + \nu + \phi\Lambda\beta}{\mu + \nu + \phi(\mu + \nu)(\mu + \gamma + \delta)}.$$

Clearly that if $\mathcal{R}_0 < 1$ then $0 < \lambda_2 < 1$, while if $\mathcal{R}_0 > 1$ then $\lambda_2 > 1$. This fact confirms that if $\mathcal{R}_0 < 1$ then the DFE E^0 is locally asymptotically stable and it is unstable if $\mathcal{R}_0 > 1$, irrespective of h . \square

To prove the local stability of DEE E^* , we need the following Schur-Cohn criterion [1, 35].

Lemma 6. [1, 35] *The roots of quadratic equation $\lambda^2 - T\lambda + D = 0$ satisfy $|\lambda_i| < 1$, $i = 1, 2$ if and only if all of the following conditions are fulfilled:*

1. $D < 1$,
2. $1 + T + D > 0$,

3. $1 - T + D > 0$.

Theorem 7. *If $\mathcal{R}_0 > 1$, then the DEE point E^* of the discrete NSFD model (3.6) is locally asymptotically stable for all $h > 0$.*

Proof. The Jacobian matrix (3.7) evaluated at the DEE point E^* is

$$J(E^*) = \begin{pmatrix} \frac{1}{a_1} & -\frac{a_4}{a_1^2} \\ \frac{a_3}{a_1 a_2} & \frac{1}{a_1^2 a_2} (a_1^2 + a_4(a_1 - a_3)) \end{pmatrix} \quad (3.9)$$

where $a_1 = 1 + \phi(\Psi^* + \mu + \nu) > 1$, $a_2 = 1 + \phi(\mu + \gamma + \delta) > 1$, $a_3 = \phi\Psi^* > 0$ and $a_4 = \frac{\phi\beta(S^* + \phi\Lambda)}{(1 + \alpha I^*)^2} > 0$. The eigenvalues of $J(E^*)$ is determined by the following quadratic equation

$$\lambda^2 - T\lambda + D = 0, \quad (3.10)$$

where $T = \text{Trace}(J(E^*)) = \frac{1}{a_1} + \frac{1}{a_1^2 a_2} (a_1^2 + a_4(a_1 - a_3))$ and $D = \text{Determinant}(J(E^*)) = \frac{a_1 + a_4}{a_1^2 a_2}$. Since $a_1 > a_3$, it is apparently that $T > 0$ and $D > 0$. We also have the following results.

1. Due to $a_1 > 1$, we get

$$\begin{aligned} D &= \frac{a_1 + a_4}{a_1^2 a_2} = \frac{1}{a_1 a_2} + \frac{a_4}{a_1^2 a_2} < \frac{1 + a_4}{a_1 a_2} \\ &= \frac{S^* + \frac{\phi S^*(\mu + \gamma + \delta)}{1 + \alpha I^*} + \frac{\phi^2 \Lambda(\mu + \gamma + \delta)}{(1 + \alpha I^*)}}{(S^* + \phi\Lambda)(1 + \phi(\mu + \gamma + \delta))} \\ &\leq \frac{S^* + \phi S^*(\mu + \gamma + \delta) + \phi^2 \Lambda(\mu + \gamma + \delta)}{S^* + \phi S^*(\mu + \gamma + \delta) + \phi^2 \Lambda(\mu + \gamma + \delta) + \phi\Lambda} \\ &< 1. \end{aligned}$$

2. It is obvious that $1 + T + D > 0$.

3. Straightforward calculations show that if $\mathcal{R}_0 > 1$ then

$$1 - T + D = \frac{\phi^2(\mu + \gamma + \delta)^2(\mu + \nu)}{a_1^2 a_2 \beta S^*} \left(1 + \frac{\phi\Lambda}{S^*}\right) [\mathcal{R}_0 - 1] > 0.$$

Hence, the conditions for the Schur-Cohn criterion in Lemma 6 are satisfied whenever $\mathcal{R}_0 > 1$. It is concluded that the DEE point E^* is locally asymptotically stable if $\mathcal{R}_0 > 1$ for any h . \square

3.3. Global stability analysis of the discrete NSFD model

This Subsection is devoted to establish the sufficient conditions for the global stability of equilibrium points of the discrete NSFD model (3.6).

Theorem 8. *If $\mathcal{R}_0 \leq 1$, then the disease free equilibrium point E^0 of the discrete NSFD model (3.6) is globally asymptotically stable for all $h > 0$.*

Proof. We first introduce a discrete Lyapunov function

$$\mathcal{U}_n = \frac{1}{\phi} \left(S^0 \varphi \left(\frac{S_n}{S^0} \right) + I_n \right) + S^0 \Psi_n, \quad (3.11)$$

where $\varphi(z) = z - 1 - \ln(z) \geq \varphi(1) = 0$. Based on the first two equations of (3.1) we obtain

$$\begin{aligned} \Delta \mathcal{U}_n &= \frac{1}{\phi} \left[S^0 \left(\varphi \left(\frac{S_{n+1}}{S^0} \right) - \varphi \left(\frac{S_n}{S^0} \right) \right) + (I_{n+1} - I_n) \right] + S^0 (\Psi_{n+1} - \Psi_n) \\ &= \frac{1}{\phi} \left[S_{n+1} - S_n + S^0 \ln \left(\frac{S_n}{S_{n+1}} \right) \right] + \Psi_n S_{n+1} - (\mu + \gamma + \delta) I_{n+1} + S^0 (\Psi_{n+1} - \Psi_n) \\ &\leq -\frac{1}{S_{n+1}} (S_{n+1} - S^0) \left(\frac{S_{n+1} - S_n}{\phi} \right) + \Psi_n S_{n+1} - (\mu + \gamma + \delta) I_{n+1} + S^0 (\Psi_{n+1} - \Psi_n) \\ &= -\frac{1}{S_{n+1}} (S_{n+1} - S^0) (\Lambda - \Psi_n S_{n+1} - (\mu + \nu) S_{n+1}) + \Psi_n S_{n+1} - (\mu + \gamma + \delta) I_{n+1} \\ &\quad + S^0 (\Psi_{n+1} - \Psi_n) \\ &= -\frac{(\mu + \nu)}{S_{n+1}} (S_{n+1} - S^0)^2 + S^0 \Psi_{n+1} - (\mu + \gamma + \delta) I_{n+1} \\ &= -\frac{(\mu + \nu)}{S_{n+1}} (S_{n+1} - S^0)^2 - (\mu + \gamma + \delta) I_{n+1} + \frac{\Lambda \beta}{(\mu + \nu)(1 + \alpha I_{n+1})} I_{n+1} \\ &= -\frac{(\mu + \nu)}{S_{n+1}} (S_{n+1} - S^0)^2 - (\mu + \gamma + \delta) \left(1 - \frac{\Lambda \beta}{(\mu + \nu)(\mu + \gamma + \delta)(1 + \alpha I_{n+1})} \right) I_{n+1} \\ &= -\frac{(\mu + \nu)}{S_{n+1}} (S_{n+1} - S^0)^2 - (\mu + \gamma + \delta) \left(1 - \frac{\mathcal{R}_0}{1 + \alpha I_{n+1}} \right) I_{n+1}. \end{aligned}$$

Obviously that if $\mathcal{R}_0 \leq 1$, then $\mathcal{U}_{n+1} - \mathcal{U}_n \leq 0$ for all $n \geq 0$, which shows \mathcal{U}_n is monotone decreasing sequence. Since $\mathcal{U}_n \geq 0$, there exists a $\lim_{n \rightarrow \infty} \mathcal{U}_n \geq 0$ and thus $\lim_{n \rightarrow \infty} (\mathcal{U}_{n+1} - \mathcal{U}_n) = 0$. Consequently we have $\lim_{n \rightarrow \infty} S_{n+1} = S^0$ and $\lim_{n \rightarrow \infty} \left(1 - \frac{\mathcal{R}_0}{1 + \alpha I_{n+1}} \right) I_{n+1} = 0$ for any h . It is straightforward to show that if $\mathcal{R}_0 \leq 1$ then $\lim_{n \rightarrow \infty} I_{n+1} = 0$. This completes the proof. \square

In the following theorem we show that E^* is globally asymptotically stable if it exists.

Theorem 9. *If $\mathcal{R}_0 > 1$, then the DEE point E^* of the discrete NSFD model (3.6) is globally asymptotically stable for all $h > 0$.*

Proof. To establish the sufficient condition for which E^* is globally stable, we apply the approach of Enatsu et al. [36]. Here we define the following discrete Lyapunov function

$$\mathcal{W}_n = S^* \varphi \left(\frac{S_n}{S^*} \right) + I^* \varphi \left(\frac{I_n}{I^*} \right) + \phi \Psi^* S^* \varphi \left(\frac{\Psi_n}{\Psi^*} \right), \tag{3.12}$$

where $\Psi^* = \Psi(I^*)$ and $\varphi(z)$ is defined as in the proof of Theorem 8. By substituting the first two equations in (3.1) into equation (3.12), we obtain

$$\begin{aligned} \Delta \mathcal{W}_n &= \mathcal{W}_{n+1} - \mathcal{W}_n \\ &= S^* \left(\varphi \left(\frac{S_{n+1}}{S^*} \right) - \varphi \left(\frac{S_n}{S^*} \right) \right) + I^* \left(\varphi \left(\frac{I_{n+1}}{I^*} \right) - \varphi \left(\frac{I_n}{I^*} \right) \right) + \phi \Psi^* S^* \left(\varphi \left(\frac{\Psi_{n+1}}{\Psi^*} \right) - \varphi \left(\frac{\Psi_n}{\Psi^*} \right) \right) \\ &= S_{n+1} - S_n + S^* \ln \left(\frac{S_n}{S_{n+1}} \right) + I_{n+1} - I_n + I^* \ln \left(\frac{I_n}{I_{n+1}} \right) \\ &\quad + \phi \Psi^* S^* \left(\frac{\Psi_{n+1}}{\Psi^*} - \frac{\Psi_n}{\Psi^*} - \ln \left(\frac{\Psi_{n+1}}{\Psi^*} \right) + \ln \left(\frac{\Psi_n}{\Psi^*} \right) \right) \\ &\leq \frac{1}{S_{n+1}} (S_{n+1} - S^*) (S_{n+1} - S_n) + \frac{1}{I_{n+1}} (I_{n+1} - I^*) (I_{n+1} - I_n) \\ &\quad + \phi \Psi^* S^* \left(\frac{\Psi_{n+1}}{\Psi^*} - \frac{\Psi_n}{\Psi^*} - \ln \left(\frac{\Psi_{n+1}}{\Psi^*} \right) + \ln \left(\frac{\Psi_n}{\Psi^*} \right) \right) \\ &= \frac{\phi}{S_{n+1}} (S_{n+1} - S^*) (\Lambda - \Psi_n S_{n+1} - (\mu + \nu) S_{n+1}) \\ &\quad + \frac{\phi}{I_{n+1}} (I_{n+1} - I^*) (\Psi_n S_{n+1} - (\mu + \gamma + \delta) I_{n+1}) \\ &\quad + \phi \Psi^* S^* \left(\frac{\Psi_{n+1}}{\Psi^*} - \frac{\Psi_n}{\Psi^*} - \ln \left(\frac{\Psi_{n+1}}{\Psi^*} \right) + \ln \left(\frac{\Psi_n}{\Psi^*} \right) \right) \\ &= -\frac{\phi(\mu + \nu)}{S_{n+1}} (S_{n+1} - S^*)^2 + \phi \Psi^* S^* \left(1 - \frac{S^*}{S_{n+1}} \right) \left(1 - \frac{\Psi_n S_{n+1}}{\Psi^* S^*} \right) \\ &\quad + \phi \Psi^* S^* \left(1 - \frac{I^*}{I_{n+1}} \right) \left(\frac{\Psi_n S_{n+1}}{\Psi^* S^*} - \frac{I_{n+1}}{I^*} \right) \\ &\quad + \phi \Psi^* S^* \left(\frac{\Psi_{n+1}}{\Psi^*} - \frac{\Psi_n}{\Psi^*} - \ln \left(\frac{\Psi_{n+1}}{\Psi^*} \right) + \ln \left(\frac{\Psi_n}{\Psi^*} \right) \right). \end{aligned} \tag{3.13}$$

By denoting $\chi_n = \frac{S_n}{S^*}$, $\xi_n = \frac{I_n}{I^*}$ and $\zeta_n = \frac{\Psi_n}{\Psi^*}$, equation (3.13) can be written as

$$\begin{aligned} \Delta \mathcal{W}_n &\leq -\frac{\phi(\mu+\nu)S^*}{\chi_{n+1}}(\chi_{n+1}-1)^2 + \phi\Psi^*S^*\left(1-\frac{1}{\chi_{n+1}}\right)(1-\zeta_n\chi_{n+1}) \\ &\quad + \phi\Psi^*S^*\left(1-\frac{1}{\xi_{n+1}}\right)(\zeta_n\chi_{n+1}-\xi_{n+1}) + \phi\Psi^*S^*(\zeta_{n+1}-\zeta_n-\ln\zeta_{n+1}+\ln\zeta_n) \\ &= -\frac{\phi(\mu+\nu)S^*}{\chi_{n+1}}(\chi_{n+1}-1)^2 - \varphi\left(\frac{1}{\chi_{n+1}}\right) - \varphi\left(\frac{\chi_{n+1}\zeta_n}{\xi_{n+1}}\right) + \phi\Psi^*S^*(\varphi(\zeta_{n+1})-\varphi(\xi_{n+1})). \end{aligned} \quad (3.14)$$

By definition of $\varphi(z)$, we can verify that

$$\begin{aligned} \varphi(\zeta_{n+1}) - \varphi(\xi_{n+1}) &= \frac{\Psi_{n+1}}{\Psi^*} - \frac{I_{n+1}}{I^*} + \ln\left(\frac{I_{n+1}}{I^*} \frac{\Psi^*}{\Psi_{n+1}}\right) \\ &\leq \frac{\Psi_{n+1}}{\Psi^*} - \frac{I_{n+1}}{I^*} + \frac{I_{n+1}}{I^*} \frac{\Psi^*}{\Psi_{n+1}} - 1 \\ &= -\frac{\alpha(I_{n+1}-I^*)^2}{I^*(1+\alpha I^*)(1+\alpha I_{n+1})} \\ &\leq 0. \end{aligned} \quad (3.15)$$

Therefore \mathcal{W}_n is monotone decreasing sequence. Using the same argument as in the proof of Theorem 8 we can show that $\lim_{n \rightarrow \infty} (\mathcal{W}_{n+1} - \mathcal{W}_n) = 0$, from which we get $\lim_{n \rightarrow \infty} S_{n+1} = S^*$ and $\lim_{n \rightarrow \infty} I_{n+1} = I^*$ for all h . Hence, we have the theorem. \square

4. Numerical simulations

To give better view of the previous analytical results, we present some numerical simulations using the proposed discrete NSFD model (3.5). For the simulations, we take initial value $S(0) = 4$, $I(0) = 0.2$, and hypothetical parameters: $\Lambda = 4$, $\mu = 0.5$, $\beta = 0.5$, $\alpha = 0.01$, $\gamma = 0.1$, $\nu = 0.2$, and $\delta = 0.1$. By calculation, the basic reproduction number is $\mathcal{R}_0 = 4.0816 > 1$. The equilibrium points of both continuous model (1.1) and discrete NSFD model (3.5) are exactly the same, namely the unstable DFE point $E^0 = (5.7143, 0.0, 2.2857)$ and the globally asymptotically stable DEE point $E^* = (1.4590, 4.2547, 1.4348)$. In Figure 1 we compare the solutions of the proposed discrete NSFD model (3.5) with those of the explicit Euler method using $h = 1$ and $h = 1.35$. It is shown that the explicit Euler method produces a periodic solution of period two for the case of $h = 1$ and a chaotic behavior for $h = 1.35$. In contrast to the explicit Euler method, the solutions of the proposed NSFD scheme (3.5) are convergent to the correct equilibrium point E^* for both $h = 1$ and $h = 1.35$. The complete dynamical behavior of the numerical results of the proposed discrete NSFD model (3.5) and the explicit Euler method with respect to h can be seen in Figure 2. Figure 2.(a–b) indicates that there exists a critical time-step size h^* such that the solution obtained by the explicit Euler method is convergent to the stable DEE point E^* if $h < h^*$. For larger time-step size, the solution may converge to a stable periodic solution of period two or that of period four, or even exhibits a chaotic behavior. On the contrary, the solutions obtained by the proposed NSFD scheme (3.5) are always convergent to the DEE point E^* for any h , see Figure 2.(c–d). These numerical simulations confirm that the dynamics of the discrete model obtained by the explicit Euler method are dependent on the time-step size, while the dynamics of the proposed discrete NSFD model (3.5) are independent of h .

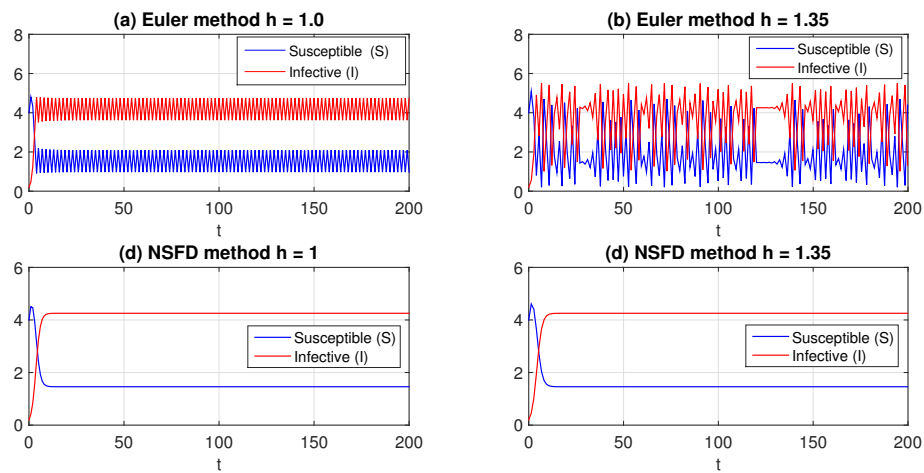


Figure 1. Numerical solutions of the SIR epidemic model (1.1) obtained by the explicit Euler method with (a) $h = 1$ and (b) $h = 1.35$; and by the proposed NSFD method (3.5) with (c) $h = 1$ and (d) $h = 1.35$.

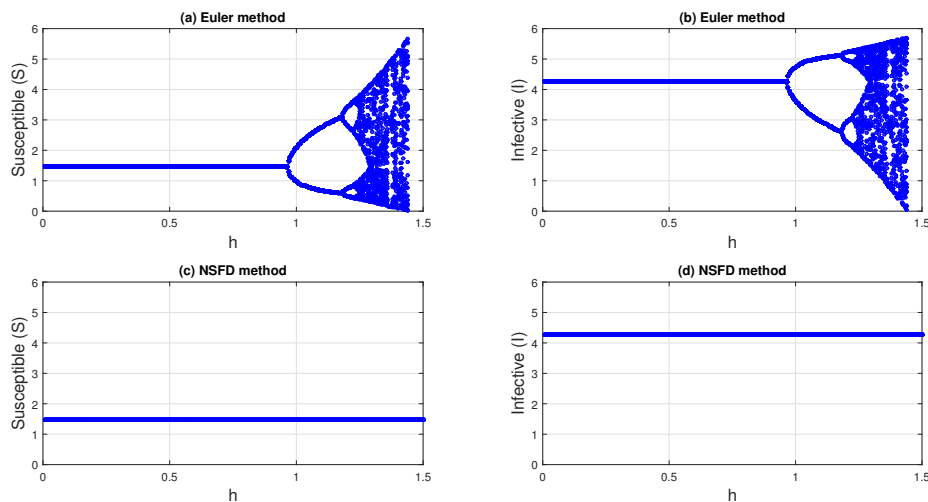


Figure 2. Bifurcation diagram in (h, S) –plane and (h, I) – plane for the discrete SIR epidemic model with $\Lambda = 4, \mu = 0.5, \beta = 0.5, \alpha = 0.01, \gamma = 0.1, \nu = 0.2$, and $\delta = 0.1$ obtained by (a–b) the explicit Euler method, and (c–d) the proposed NSFD method (3.5).

Next, using the same parameter values as before, we compare the numerical solutions obtained by the NSFD scheme (1.2) [18] and our proposed NSFD scheme (3.5), see Figure 3. Here, the denominator function for the NSFD scheme (1.2) is $\phi = \frac{1 - \exp(\mu h)}{\mu}$. As stated in the Introduction, the NSFD scheme proposed in [18] is dynamically consistent only for restrictive time-step size. Indeed, according to the analytical results in [18], the NSFD scheme (1.2) is dynamically-consistent if $\phi^* < 0.9486$ which is equivalent to $h < 1.2860$. Figure 3 confirms this phenomenon. If we take $h = 1.5$ then the numerical solution obtained by the NSFD scheme (1.2) does not converge to the DEE point but it goes to a periodic solution of period two, see Figure 3.(a). If we further increase the

time-step size ($h = 2$) then we get a chaotic solution, see Figure 3.(b). On the other hand, the proposed NSFD scheme (3.5) preserves the stability of the DEE point, even for relatively large h , see Figure 3.(c–d).

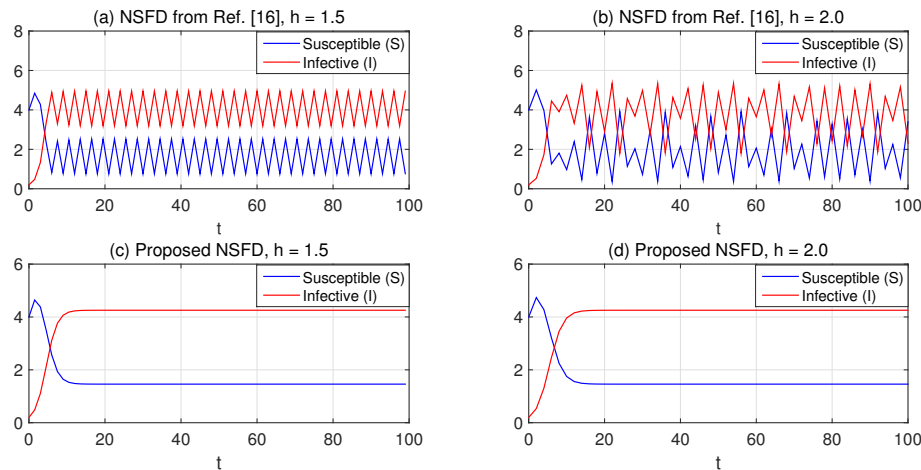


Figure 3. Numerical solutions of the SIR epidemic model (1.1) obtained by the NSFD scheme (1.2) and the proposed NSFD scheme (3.5).

Finally, we perform simulation using parameters $\Lambda = 1, \mu = 0.5, \beta = 0.25, \alpha = 0.01, \gamma = 0.1, \nu = 0.2, \delta = 0.1$, and time step size $h = 0.1$ with initial value $S(0) = 6$ and $I(0) = 1$. The reproduction number in this case is $\mathcal{R}_0 = 0.5102 < 1$. Hence, the DFE point $E^0 = (1.4286, 0.0, 0.5714)$ is asymptotically stable while the DEE point does not exist. The solution obtained by the proposed NSFD scheme (3.5) confirms the stability of the DFE point, see Figure 4.(a). For comparison, we also plot the numerical solutions obtained by the ordinary differential equations (ODE) solvers in MATLAB, namely ode23s (the 2nd order modified Rosenbrock), ode23t (the trapezoidal rule using a “free” interpolant) and ode45 (the Runge-Kutta Dormand-Prince method of order (4,5)) with their default tolerance. The y-axis (susceptible and infective sub-populations) in this figure is plotted in the logarithmic scale. Notice that the logarithmic function $\log(y)$ is defined only for $y > 0$. Hence, if the solution (susceptible or infective sub-population) is negative then the figure cannot be plotted (it is ignored by MATLAB). Figure 4.(a) shows that the solution given by the proposed NSFD scheme is convergent to the DFE point and is positive for all t . We observe in Figure 4.(b-d) that solutions obtained by all three MATLAB ODE solvers go to the DFE point but the infective subpopulation $I(t)$ is discontinuous at some points, showing that all three MATLAB ODE solvers produce unrealistic negative solutions. Although the tolerances of MATLAB ODE solvers are reduced such that $\text{AbsTol} = 10^{-12}$ and $\text{RelTol} = 10^{-12}$, we still observe that the three MATLAB ODE solvers produce unrealistic negative solutions.

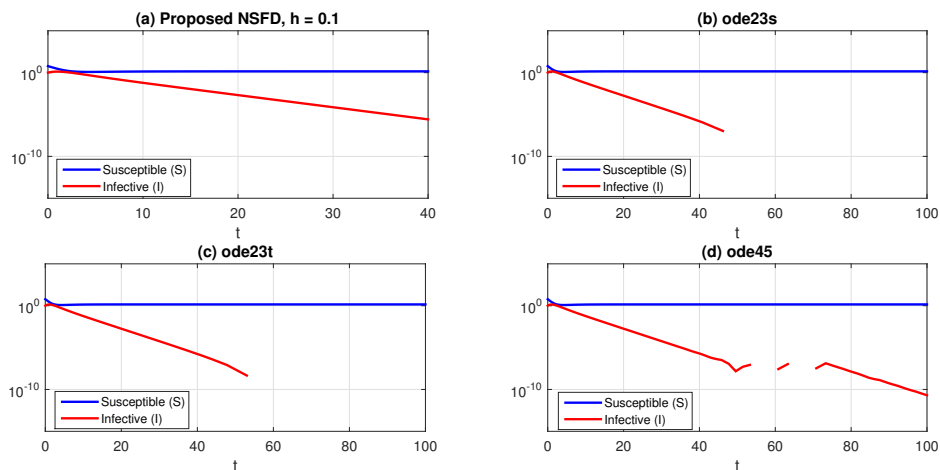


Figure 4. Numerical solutions of the SIR epidemic model (1.1) obtained by the proposed NSFD scheme (3.5) and three ODE solvers in MATLAB (ode23s, ode23t and ode45).

5. Conclusions

In this article we have proposed and analyzed a dynamically-consistent discrete SIR epidemic model with saturated incidence rate and vaccination. The discrete model is constructed using the NSFD method. In contrast to the discrete NSFD model available in literature, we constructed the discrete NSFD model by applying a nonlocal approximation for the nonlinear terms and choose a suitable denominator function. The denominator function is derived in such way that the NSFD scheme satisfies the exact boundedness of solutions. The existence conditions of all equilibrium points of the proposed discrete NSFD model are derived and the sufficient conditions for which the equilibrium points are locally and globally stable have also been established. We have shown that the proposed discrete NSFD model has exactly the same dynamics as those of continuous model irrespective of the time-step size. These qualitative properties have been confirmed by our numerical simulations. Furthermore, our numerical simulations showed that the discrete model obtained by the explicit Euler method and the NSFD scheme proposed in other literatur is dynamically-consistent with the related continuous model only when the time-step size is relatively small. The three MATLAB ODE solvers (ode23s, ode23t, ode45) may fail to produce realistic solutions, i.e., the solutions may be negative.

Acknowledgments

This research is funded by FMIPA-UB via PNBP-University of Brawijaya according to DIPA-UB No. DIPA-023.17.2.677512/2020, under contract No. 12/UN10.F09/PN/2020.

Conflict of interest

All authors declare no conflict of interest.

References

1. F. Brauer, C. Castillo-Chavez, *Mathematical Model in Population Biology and Epidemiology*, 2nd edition, Springer-Verlag, New York, 2010.
2. F. Brauer, Mathematical epidemiology: Past, present, and future, *Infect. Dis. Modell.*, **2** (2017), 113–127.
3. M. Martcheva, *An Introduction to Mathematical Epidemiology*, Springer, New York, 2015.
4. T. T. Yusuf, F. Benyah, Optimal control of vaccination and treatment for an SIR epidemiological model, *World J. Modell. Simul.*, **8** (2012), 194–204.
5. V. Capasso, G. Serio, A generalisation of the Kermack-McKendrick deterministic epidemic model, *Math. Biosci.*, **42** (1978), 43–61.
6. J. Zhang, J. Jia, X. Song, Analysis of an SEIR epidemic model with saturated incidence and saturated treatment function, *Sci. World J.*, **2014** (2014), Article ID 910421.
7. R. Xu, Z. Ma, Z. Wang, Global stability of a delayed SIRS epidemic model with saturation incidence and temporary immunity, *Comput. Math. Appl.*, **59** (2010), 3211–3221.
8. S. Jana, S. K. Nandi, T. K. Kar, Complex dynamics of an SIR epidemic model with saturated incidence rate and treatment, *Acta Biotheoretica*, **64** (2016), 65–84.
9. K. S. Mathur, P. Narayan, Dynamics of an SVEIRS epidemic model with vaccination and saturated incidence rate, *Int. J. Appl. Comput. Math.*, **4** (2018), Article number: 118.
10. J. Liu, Bifurcation analysis for a delayed SEIR epidemic model with saturated incidence and saturated treatment function, *J. Biol. Dyn.*, **13** (2019), 461–480.
11. A. A. Lashari, Optimal control of an SIR epidemic model with a saturated treatment, *Appl. Math. Inf. Sci.*, **10** (2016), 185–191.
12. J. K. Ghosh, U. Ghosh, M. H. A. Biswas, S. Sarkar, *Qualitative analysis and optimal control strategy of an SIR Model with saturated incidence and treatment*, *Differential Equations and Dynamical Systems*, Available from: <https://doi.org/10.1007/s12591--019--00486--8>.
13. I. A. Baba, R. A. Abdulkadir, P. Esmaili, Analysis of tuberculosis model with saturated incidence rate and optimal control, *Physica A: Stat. Mech. Appl.*, **540** (2020), Article number: 123237.
14. S. P. Rajasekar, M. Pitchaimani, Q. Zhu, Dynamic threshold probe of stochastic SIR model with saturated incidence rate and saturated treatment function, *Physica A: Stat. Mech. Appl.*, **535** (2019), Article number: 122300.
15. S. P. Rajasekar, M. Pitchaimani, Q. Zhu, Progressive dynamics of a stochastic epidemic model with logistic growth and saturated treatment, *Physica A: Stat. Mech. Appl.*, **538** (2020), Article number: 122649.
16. S. P. Rajasekar, M. Pitchaimani, Ergodic stationary distribution and extinction of a stochastic SIRS epidemic model with logistic growth and nonlinear incidence, *Appl. Math. Comput.*, **377** (2020), Article number: 125143.
17. T. Khan, Z. Ullah, N. Ali, G. Zaman, Modelling and control of the hepatitis B virus spreading using an epidemic model, *Chaos. Solitons Fractals*, **124** (2019), 1–9.

18. M. T. Hoang, O. F. Egbelowo, On the global asymptotic stability of a hepatitis B epidemic model and its solutions by nonstandard numerical scheme, *Boletín de la Sociedad Matemática Mexicana*, **2020** (2020), Available from: <https://doi.org/10.1007/s40590-020-00275-2>.
19. J. E. Macías-Díaz, N. Ahmed, M. Rafiq, Analysis and nonstandard numerical design of a discrete three-dimensional hepatitis B epidemic model, *Mathematics*, **2019** (2019), Article ID: 1157.
20. A. Suryanto, A dynamically consistent nonstandard numerical scheme for epidemic model with saturated incidence rate, *Int. J. Math. Comput.*, **13** (2011), 112–123.
21. A. Suryanto, *Stability and bifurcation of a discrete SIS epidemic model with delay*, Proceedings of the 2nd International Conference on Basic Sciences, Malang, Indonesia, (2012), 1–6.
22. Z. Hu, Z. Teng, H. Jiang, Stability analysis in a class of discrete SIRS epidemic models, *Nonlinear Analysis: Real World Appl.*, **13** (2012), 2017–2033.
23. R. Mickens, *Non standard finite difference models of differential equations*, World Scientific, Singapore, 1994.
24. Q. Cui, J. Xu, Q. Zhang, K. Wang, An NSFD scheme for SIR epidemic models of childhood diseases with constant vaccination strategy, *Advances Difference Equations*, **2014** (2014), Article number: 172.
25. Q. Cui, X. Yang, Q. Zhang, An NSFD scheme for a class of SIR epidemic models with vaccination and treatment, *J. Difference Equations Appl.*, **20** (2014), 416–422.
26. Q. Cui, Q. Zhang, Global stability of a discrete SIR epidemic model with vaccination and treatment, *J. Difference Equations Appl.*, **21** (2015), 111–117.
27. K. Hattaf, A. A. Lashari, B. E. Boukari, N. Yousfi, Effect of discretization on dynamical behavior in an epidemiological model, *Differential Equations Dyn. Syst.*, **23** (2015), 403–413.
28. P. R. S. Rao, K. V. Ratnam, M. S. R. Murthy, Stability preserving non standard finite difference schemes for certain biological models, *Int. J. Dyn. Control*, **6** (2018), 1496–1504.
29. I. Darti, A. Suryanto, M. Hartono, Global stability of a discrete SIR epidemic model with saturated incidence rate and death induced by the disease, *Comm. Math. Biol. Neurosci.*, **2020** (2020), Article ID 33.
30. I. Darti, A. Suryanto, Dynamics of a SIR epidemic model of childhood diseases with a saturated incidence rate: Continuous model and its nonstandard finite difference discretization, *Mathematics*, **8** (2020), 1459.
31. I. Darti, A. Suryanto, Stability preserving non-standard finite difference scheme for a harvesting Leslie-Gower predator–prey model, *J. Difference Equations Appl.*, **21** (2015), 528–534.
32. I. Darti, A. Suryanto, Dynamics preserving nonstandard finite difference method for the modified Leslie-Gower predator–prey model with Holling–type II functional response, *Far East J. Math. Sci.*, **99** (2016), 719–733.
33. M. S. Shabbir, Q. Din, M. A. Khan, M. A. Khan, K. Ahmad, A dynamically consistent nonstandard finite difference scheme for a predator–prey model, *Advances Difference Equations*, **2019** (2019), Article number: 381.
34. Q. A. Dang, M. T. Hoang, Complete global stability of a metapopulation model and its dynamically consistent discrete models, *Qual. Theory Dyn. Syst.*, **18** (2019), 461–475.

-
35. S. Elaydi, *An Introduction to Difference Equations*, 3rd edition, Springer-Verlag, New York, 2005.
36. Y. Enatsu, Y. Nakata, Y. Muroya, G. Izzo, A. Vecchio, Global dynamics of difference equations for SIR epidemic models with a class of nonlinear incidence rates, *J. Difference Equations Appl.*, **18** (2012), 1163–1181.



AIMS Press

©2021 the Author(s), licensee AIMS Press. This is an open access article distributed under the terms of the Creative Commons Attribution License (<http://creativecommons.org/licenses/by/4.0>)